The novel cargo Alcadein induces vesicle association of kinesin-1 motor components and activates axonal transport

Yoichi Araki, Takanori Kawano, Hidenori Taru, Yuhki Saito, Sachiyo Wada, Kanako Miyamoto, Hisako Kobayashi, Hiroyuki O. Ishikawa, Yu Ohsugi, Tohru Yamamoto, Kenji Matsuno, Masataka Kinjo, and Toshiharu Suzuki

Supplementary information (Sup_1.pdf)

Supplementary Materials

cDNA cloning and plasmid construction. The mKLC1-N cDNA encoding the amino-terminal 200 amino acids and the mKLC1-C cDNA encoding the carboxyl-terminal 342 amino acids were prepared by PCR (see Figure 1A). mKLC1-C cDNA was subcloned into the pcDNA3.1 vector at the *HindIII*/*Xba*I sites to produce pcDNA3.1-mKLC1-C. Sequences encoding FLAG- or GFP-tags were inserted at the 5'-terminus of the cDNAs to produce pcDNA3.1-FLAG-mKLC1, pcDNA3.1-FLAG-mKLC2, pcDNA3.1-FLAG-mKLC1-N, pcDNA3.1-FLAG-mKLC1-C, and pcDNA3.1-GFP-mKLC1. Human APP695 and Alcα1 cDNA (Araki *et al*., [2003] *J. Biol. Chem*. **278**, 49448-49458) were inserted into pcDNA3.1-GFP at the *HindIII/XbaI* sites to produce pcDNA3.1-hAPP695-GFP and pcDNA3.1-hAlcα1-GFP, or into pcDNA3.1c-Venus (supplied by Dr. A. Miyawaki) at the *Hind*III/*Xba*I sites to produce pcDNA3.1hAPP695-Venus and pcDNA3.1hAlcα1-Venus (Nagai *et al*., [2002] *Nat. Biotech.* **20**, 87-90). Venus is a brighter version of YFP. pcDNA3.1hAPP695, pcDNA3-AlcαICD and pcDNA3-AlcαICD/NPAA were prepared as described previously (Araki *et al*., [2004] *J. Biol. Chem.* **279**, 24343-24354), and pcDNA3-AlcαICD/AWAA was prepared by PCR using pcDNA3-AlcαICD. FLAG-X11L, FLAG-FE65, and FLAG-JIP1b were prepared as described previously (Taru *et al*., [2002b] *J. Biol. Chem.* **277**, 20070-20078). JIP1bΔC11 lacking the carboxyl-terminal 11 amino acids of human JIP1b was prepared and inserted into the pcDNA3.1 vector.

Antibodies. The rabbit anti-APP (G369) (Oishi *et al*., [1997] *Mol. Med.* **3**, 111-123) and anti-Alcα (UT83) (Araki *et al*., [2003] *J. Biol. Chem.* **278**, 49448-49458) antibodies have been characterized. The guinea pig anti-Alcα polyclonal antibody co190 was raised against the mouse Alcα cytoplasmic region (amino acids 853-960 of mouse Alcα1) fused to GST. Polyclonal antibodies were affinity-purified. Monoclonal antibodies specific for the kinesin heavy chain (H2, Chemicon International), PDI (1D3, Stressgen Biotechnologies), GM130 (clone no. 35, BD Bioscience), SYT (clone no. 41, BD Biosciences), Neuronal Class III β-tubulin (TUJ1, CRP INC), synaptophysin (SY38, DAKO), and FLAG (M2, Sigma), and a rabbit polyclonal antibody for APP (αAPP/C, cat. no. A8717

Sigma), were purchased. The 3A10 monoclonal antibody against the neurofilament-associated antigen was obtained from the Developmental Studies Hybridoma Bank. The rabbit anti-APPL polyclonal antibody (Luo *et al*., [1990] *J. Neurosci.* **10**, 3849-3861) and anti-synaptic vesicle monoclonal antibody (CSP) (Zinsmaier *et al*., [1994] *Science* **263**, 977-980) were provided by Drs. White and Zinsmaier, respectively. The specificity of co190, UT109, and UT110 is shown in Figure S9. UT135 was raised against a peptide (amino acids 839-851 of human Alcα1), which recognizes β-Alcα specifically, but does not recognize β-Alcβ or β-Alcγ derived from the other Alc families (Hata, S., Araki, Y. and Suzuki, T., unpublished observation). The rabbit anti-JIP1b polyclonal antibody (UT72) was raised against a GST-fusion protein of mouse JIP1b amino acids 1-470.

Total internal reflectance fluorescence (TIRF) microscopy analysis. CAD cells and HEK293 cells cultured on a coverglass chamber slide coated with poly L-lysine were transfected with the indicated plasmid for 18 h. Mouse cortical neuron cultures were prepared from embryonic day 16 C57BL/6 mice. Dissociated cells (1 x10^4~10^5 cells) were cultured in medium for 5 days (Brewer *et al*., [1993] *J. Neurosci.* Res. **35**, 567-576) and transfected with the indicated plasmids in calcium phosphate for 0.5 h and cultured for 24 h. We determined the velocity of vesicles using the Stokes-Einstein formula as follows: $D = kT/6\pi\eta_0 d$, $V^2 = 4Dt$, where D, diffusion coefficient [m^2S^{-1}]; k, Boltzmann constant [$m^2kg{\cdot}s^{-2}K^{-1}$]; T, temperature [K]; d, Stokes radius [m]; η_0, viscosity [Pa·s]; t, Time [s]; V, velocity [$m{\cdot}s^{-1}$]. The values for the Stokes radius and viscosity were estimated as: d = 0.3 [μm] (3 x 10^{-7} [m]), η_0 = 5 x 10^{-3} [Pa·s] (Haak, Kleinhans & Ochs, [1976] *J. Physiol.* **263**, 115-137). Vesicles moving with a velocity below 0.38 μm/sec (below approximately 0.4 μm/sec) are indistinguishable from those moving by Brownian movement. Vesicles present in the TIRF area, i.e., within approximately 100 nm of the plasma membrane, were counted using the "count objects" function of Metamorph 6.1.

In vitro binding assay and surface plasmon resonance analysis. For the *in vitro* binding assay, cDNA encoding mouse KLC1 was subcloned into pGEX-6P-1 (GE Healthcare). The GST region of the fusion protein was removed by cleavage with PreScission Protease (GE Healthcare), and mKLC1 was purified for use in the binding assay. In surface plasmon resonance analysis, purified GST-Alcαcyt was immobilized on a CM5 sensor chip using an anti-GST antibody. The indicated concentration of purified KLC1 was assayed at a flow rate of 5 μl/min. The sensorgrams shown in Figure S3B in Sup_1.pdf are the result of subtraction of a blank sensorgram in which GST protein alone was assayed as a control.

Preparation of cell lysates and brain membrane fractions for Coimmunoprecipitation and Western blot assays. HEK293 cells (~5 x 10^6) were transfected with the indicated plasmid as described (Araki *et al*., 2003), cultured for 24 h, and lysed on ice in HBST buffer (10 mM Hepes-NaOH [pH 7.4], 0.5% [v/v] Triton X-100, 150 mM NaCl, 5 μg/ml leupeptin, 5 μg/ml pepstatin A, and 5 μg/ml chymostatin). After centrifugation (15,000 x g for 10 min),

antibody was added to the supernatant of the HBST lysate. An adult mouse brain (male, C57BL/6, 8 weeks old) was homogenized on ice in 8 volumes of buffer A (10 mM Hepes-NaOH [pH 7.4] containing 0.32 M sucrose, 5 μg/ml leupeptin, 5 μg/ml pepstatin A, and 5 μg/ml chymostatin) using a Teflon homogenizer (clearance 0.2 μm). After centrifugation (1,000 x g for 10 min), the post-nuclear supernatant was further centrifuged at 100,000 x g for 60 min. The precipitated membrane fraction was solubilized in 8 volumes of HBST buffer and centrifuged at 100,000 x g for 60 min. Antibody was added to the HBST supernatant.

Immunostaining of mouse peripheral nerves

Mouse adult sciatic nerves and a peripheral nerve of mouse embryos (11.5 d.p.c) were fixed in 4% (w/v) paraformaldehyde in PBS for 3 h at 4 ^{o}C, washed with PBS, submerged in 30% (w/v) sucrose in PBS, embedded and frozen in Tissue-Tek (Sakura Finetec Co.), and sectioned with a cryostat (MICROM). The sections were incubated with co190 (1:3,000), anti-APP (Sigma; 1:3,000), 3A10 (1:2,000), anti-neuronal Class III β-tubulin TUJ1 (1:2,000), or SY38 anti-synaptophysin (1:1,000) and visualized using Cy3-conjugated anti-guinea pig, FITC-conjugated anti-rabbit, and Cy5-conjugated anti-mouse antibodies, respectively (donkey, minimum cross-reacting; Jackson). The immunostained nerves were observed using a Radiance 2100 confocal laser scanning microscope (BioRad) or an LSM510 (Carl Zeiss).

Supplementary Figure Legends

Figure S1. Schematic diagram of KLC1 proteins encoded by cDNA isolated in a yeast two-hybrid screen. The yeast two-hybrid system used in this study has been described previously (Tomita *et al*, [1999] *J. Biol. Chem.* 274, 2243-2254; Araki *et al*. [2003] *J. Biol. Chem.* 278, 49448-49458). Briefly, the mouse brain MATCH-MAKER cDNA library (Clontech) was screened with a bait composed of cDNA encoding the cytoplasmic domain of Alcα (amino acids 872-969 of mouse Alcα1). The screen yielded 11 cDNA clones that contained entire or partial open reading frames of KLC1 and one cDNA clone that contained a partial open reading frame of KLC2. All clones included the carboxyl terminal half of KLC.

Figure S2. Expression and characterization of Alcα and kinesin-1 components.

(A) Expression and characterization of Alcα and kinesin-1 components in HEK293 cells and mouse brain. Lysates of HEK293 cells transiently co-transfected with (+) or without (-) pcDNA3-hAlcα1 in the presence (+) or absence (-) of pcDNA3.1-mKLC1, and mouse brain lysates were analyzed by Western blotting with UT83, UT109, UT110, and H2 (anti-KHC). Vector alone (-) is indicated. Slower (arrow 1) and faster (arrow 2) migrating forms of Alcα1 are indicated. **(B)** Deglycosylation of Alcα. HEK293 cells (~5 x 10^6) transiently transfected with pcDNA3-hAlcα1

and pcDNA3.1-mKLC1 (left panel) and adult mouse brain (male, C57BL/6, 8 weeks old) (right panel) were lysed in 4 ml of HBST buffer. The lysates were denatured in a buffer containing 0.5% (w/v) SDS and 1% (v/v) 2-mercaptoethanol by boiling for 10 min. The samples were treated with endoglycosidase H (Endo H), which removes the high-mannose form of *N*-glycan, *N*-glycosidase F (PNGase F), which removes both high-mannose and complex *N*-glycans, or without enzymes (control) according to the manufacturer's protocol (New England BioLabs). Alcα in lysates was analyzed by Western blotting with the anti-Alcα antibody UT83. Arrow 1, Alcα1 with complex *N*-glycosylation; Arrow 2, Alcα1 with high-mannose-type *N*-glycosylation; Arrow 3, non-glycosylated Alcα1.

Figure S3. Kinetic analysis of the association of KLC1 with Alcα.

(A) Stoichiometry of Alcα-KLC binding. (Left) Increasing amounts (0-400 nM) of purified KLC1 were incubated with a constant amount (50 nM) of GST-Alcαcyt or GST alone for 60 min, and KLC1 bound to Alcαcyt was recovered on glutathione beads. Bound (B) and unbound (UB) KLC1 was quantified by Western blotting with an anti-KLC1 antibody (UT109). GST-Alcαcyt was quantified by Western blotting with UT83. (Right) Dose-response curve of KLC1-binding to GST-Alcαcyt. Scatchard analysis was performed to determine the K_D value using linear regression, R^2=0.96. "B" indicates bound and "F" indicates free (unbound) KLC1. **(B)** Surface plasmon resonance (SPR) analysis of the interaction between Alcαcyt and KLC1. The indicated concentrations (nM) of purified KLC1 were allowed to interact with GST-Alcαcyt immobilized on a sensor chip for the indicated times (sec). Resonance units (RU) are shown.

Figure S4. Kinesin-1-dependent anterograde transport of Alcα cargo in living neurons.

(A) Anterograde movement of Alcα1 cargo in an axon. Mouse primary cultured cortical neurons expressing Alcα1-Venus were observed using TIRF microscopy (panel 1). Vesicle movements in the dotted square were tracked with time-lapse imaging and are indicated with colored lines and numbers (see Movie 2, part 1 in Sup_3.mov). Scale bar, 5 μm. **(B)** Kinesin-1-dependent transport of Alcα1 cargo in neurons. Mouse primary cultured cortical neurons expressing Alcα1-Venus in which KLC1 and KLC2 expression has been knocked-down using siRNA were observed using TIRF microscopy (panel 1). Vesicle movements in the dotted square were tracked with time-lapse imaging and are indicated with colored lines and numbers (see Movie 2, part 2 in Sup_3.mov). Scale bar, 5 μm. **(A-B)** Red and orange lines indicate tracks of anterograde transport, blue lines indicate tracks of retrograde transport, and green spots indicate stationary vesicles moving at less than 0.4 μm/sec (panel 1). Alcα1 cargo vesicles transported anterogradely ("A") and retrogradely ("R"), and stationary vesicles ("S") in 24 neurons were counted with Metamorph software and the fraction of the total number of vesicles (%) is indicated (panel 2). Distribution (%) of anterograde (red) and retrograde (blue) transport velocity of Alcα1-cargo

was indicated with stationary vesicles (green) defined as having a velocity less than 0.4 μm/sec (panel 3).

Figure S5. Anterograde transport of Alcα1 and APP containing vesicles in same single cell. (A) Anterograde movement of Alcα1 and APP containing vesicles in an axon. Differentiating CAD cells expressing APP-GFP and Alcα1-mRFP were observed using TIRF microscopy with prism-based 3CCD camera, ASHURA (Hamamatsu Photonics K.K., Hamamatsu Japan), to measure two wavelengths (Excitation 488 nm/ emission 500-550 nm for GFP and excitation 594 nm/ emission 610-690 nm for RFP) simultaneously (panel 1). **(B)** Kinesin-1-dependent transport of Alcα1 and APP containing vesicles in an axon. Differentiating CAD cells expressing APP-GFP and Alcα1-mRFP in which KLC1 and KLC2 expression has been knocked-down using siRNA were observed as described above (panel 1). (**A,B**) Vesicle movements were tracked with time-lapse imaging and are indicated with green (APP-GFP) and red (Alcα1-mRFP) lines and numbers (see Movie 6 in Sup_7.mov) (panel 2). Anterogradely transported APP-GFP and Alcα1-mRFP vesicles were counted with Metamorph software and distribution (%) of transport velocity of APP (green)- and Alcα1(red)- containing vesicles is indicated (panel 3). Scale bar, 5 μm.

Figure S6. Alcα1 and APP cargo in mouse embryonic peripheral nerves. Vesicles containing APP (aAPP/C), Alcα1 (Co190), and synaptophysin/SYP (SY38) in a peripheral nerve of a mouse embryo (11.5 d.p.c) were immunostained as described in Supplementary information (Sup_1.pdf). Merged signals are shown in the left panels. Yellow arrowheads indicate vesicles containing both APP and Alcα. Scale bar, 5 μm.

Figure S7. Competitive suppression of Aβ generation from APP by Alcα1.

(A) In vitro inhibition of Aβ generation by Alcα. HEK293 cells were transiently co-transfected with pcDNA3-hAPP695sw (0.5 μg) and 0, 0.1, 0.5, or 1.0 μg pcDNA3.1-Alcα1. To standardize the plasmids, pcDNA3.1 vector (-) was added to yield 1.5 μg of total plasmid. Transfection with 0.5 μg plasmid (+) and vector alone (-) is indicated. The cells were treated with 2 μM DAPT (γ-secretase inhibitor) for 24 h to accumulate intracellular CTFs. The cells were washed with buffer H and disrupted in detergent-free buffer by passing through a 27 gauge needle, as described (Araki *et al*., [2004] *J. Biol. Chem*. 279, 24343-24354). The sample was centrifuged (100,000 x g for 1h) and the resulting membrane fraction was incubated at 37 ^{o}C for 2 h, as described (Araki *et al*. [2004]), and then analyzed by Western blotting for APPsw (APP/C), Alcα1 (UT-83), Aβ40 and Aβ42 (6A10), and β-Alcα (UT135). The two upper rows show the intracellular content of APPsw and Alcα1. The two lower rows show the generation of Aβ40 and Aβ42 from APP, and β-Alcα from Alcα1 after incubation. Increased expression of Alcα1suppresses the generation of Aβ from APP because it is a competitive substrate of the γ-secretase complex, which cleaves both APP and Alcα1 in a coordinated fashion (Araki *et al*., [2004] *J. Biol. Chem*. 279, 24343-24354). Aβ40 migrates more slowly than Aβ42 on this type of gel (Qi-Takehara *et al*., [2001]

J.Neurosci. 125, 436-445). (**B**) The relative ratios of (Aβ/APP) to Aβ40 (left columns) and Aβ42 (right columns) following the incubation are indicated. The data (n=3) were analyzed by one-way analysis of variance followed by Tukey's test (*, $P < 0.05$; **, $P < 0.01$; ***, $P < 0.005$).

Figure S8. Diagrams of the vesicle association of kinesin-1 components induced by Alcα in anterograde transport of the vesicles, and proposed mechanism of cargo activation of the kinesin-1 motor. (A) Vesicle association of kinesin-1 components by Alcα. Alcα directly associates with KLC using specific WD motifs (see Figure 1G), potentially the first step in kinesin-1 motor component vesicle association. The Alcα-kinesin-1 motor complex may be recruited to a microtubule and transported to nerve terminal on a microtubule track. When the Alcα cargo reaches its destination, KLC releases the Alcα cargo, and Alcα is exposed on the plasma membrane. **(B)** APP containing vesicles associated with the kinesin-1 motor may compete with Alcα-cargo and/or its cleavage product AlcαICD. APP containing vesicles may be transported *via* JIP1b with (left lower) or without (left upper) an unidentified cargo receptor (X) for kinesin-1. APP-containing vesicles may be released by generation of AlcαICD (middle upper) and/or replaced by Alcα cargo by direct interaction of KLC with Alcα (middle lower). Such competition results in release and aggregation of APP containing vesicles. APP in detached vesicles is likely to be cleaved more efficiently than that in actively transporting vesicles (right). ζ, primary cleavage site of Alcα; β, β-cleavage site of APP; γ, γ-cleavage site of Alcα and APP (Araki *et al*. [2004] *J. Biol. Chem.* **279**, 24343-24354; Gandy [2005] *J. Clin. Invest.* **115**, 1121-1129).

Figure S9. Antibody specificities.

(A) Antibody specificity. Mouse brain lysates (20 μg protein) were analyzed by Western blotting with anti-Alcα (co190), anti-KLC1 (UT109), and anti-KLC2 (UT-110) antibodies with (+) or without (-) antigen peptide (10 μM). The asterisk indicates a glycosylated form of CTF1, the C-terminal fragment of Alcα cleaved at the primary cleavage site (Araki *et al*., [2004] *J. Biol. Chem.* **279**, 24343-24354.). **(B)** Absence of cross reactivity of anti KLC antibodies. Mixtures of antibody containing UT109 (0.2 μg/ml) and UT110 (0.2 μg/ml) were used to detect KLC1 and KLC2 in mouse brain lysates (20 μg protein) by Western blotting in the presence (KLC1 or KLC2) or absence (-) of antigen peptides (10 μM). **(A, B)** Numbers (220, 97, 66, and 30) indicate molecular weight (kDa) standards and "F" indicates the dye front of the gel.

Supplementary Movies

Movie 1 (Sup_2. mov). Kinesin-1-dependent anterograde transport of Alcα cargo in living CAD cells. Part 1, Transport of Alcα1-GFP in differentiating CAD cells. Part 2, Inhibition of Alcα1-GFP transport in

differentiating CAD cells in which KLC1 and KLC2 expression is suppressed. Part 3, Inhibition of Alcα1-GFP transport in differentiating CAD cells expressing JIP1b. Part 4, Lack of inhibition of Alcα1-GFP transport in differentiating CAD cells expressing JIP1bΔC11, which is unable to interact with KLC. Scale bar, 5 μm. See Figure 2 legend.

Movie 2 (Sup_3.mov). Anterograde transport of Alcα1 cargo in mouse primary cultured cortical neurons expressing Alcα1-Venus. Part 1, Transport of Alcα1-Venus in a primary cultured neuron. Part 2, Inhibition of Alcα1-Venus transport in a neuron in which KLC1 and KLC2 expression is suppressed. See Figure S4 legend.

Movie 3 (Sup_4.mov). Microtubule-dependent movement of Alcα1 cargo in HEK293 cells. Part 1, Movement of Alcα1-Venus. Part 2, Inhibition of Alcα1-Venus by nocodazole treatment. HEK293 cells expressing Alcα1-Venus and KLC1 were observed using TIRF microscopy in the presence (Part 2) or absence (Part 1) of nocodazole (1 μM). Part 3, Alcα1-mRFP and YFP-tubulin expressed in HEK293 cells with KLC1. Vesicle movements were tracked with time-lapse imaging.

Movie 4 (Sup_5.mov). Vesicle association of kinesin-1 components induced by Alcα1 cargo and vesicle transport. Differentiating CAD cells expressing GFP-KLC1 with (Part 2) or without (Part 1) Alcα1 were observed by TIRF microscopy. Differentiating CAD cells expressing GFP-KHC with (Parts 4 and 5) or without (Part 3) KLC1 in the presence (Part 5) or absence (Parts 3 and 4) of Alcα1. Differentiating CAD cells expressing GFP-KHC with KLC (Part 6) or GFP-KLC (Part 7) in the presence of JIP1b and APP. Vesicle movements were tracked with time-lapse imaging. Scale bar, 5 μm. See Figure 3 legend.

Movie 5 (Sup_6.mov). Axonal transport of APP-GFP in differentiating CAD cells and its suppression by expression of Alcα1 and AlcαICD. Part 1, Transport of APP-GFP in differentiating CAD cells. Part 2, Inhibition of APP-GFP transport in differentiating CAD cells in which KLC1 and KLC2 expression is suppressed. Part 3, Suppression of APP-GFP transport in differentiating CAD cells by Alcα1 expression. Part 4, Suppression of APP-GFP transport in differentiating CAD cells expressing AlcαICD. Part 5, Lack of suppression of APP-GFP transport in differentiating CAD cells expressing AlcαICD(AWAA), which is unable to interact with KLC. Cells were observed using TIRF microscopy. Scale bar, 3 μm. See Figure 4 legend.

Movie 6 (Sup_7.mov). Anterograde transport of Alcα1 and APP containing vesicles in same single cell. Part 1, Transport of APP-GFP and Alcα1-mRFP in differentiating CAD cells. Part 2, Inhibition of APP-GFP and Alcα1-mRFP transport in differentiating CAD cells in which KLC1 and KLC2 expression is suppressed. Cells were observed using TIRF microscopy with 3CCD camera, ASHURA. Scale bar, 5 μm. See Figure S5 legend.

Movie 7 (Sup_8.mov). *Drosophila* alcadein (dAlc) interferes with motor neuron function when expressed in *Drosophila* larvae. Movement of *elav*-Gal4/+ and *elav*-Gal4/UAS-dAlc third instar larvae. See Figure 7 legend.

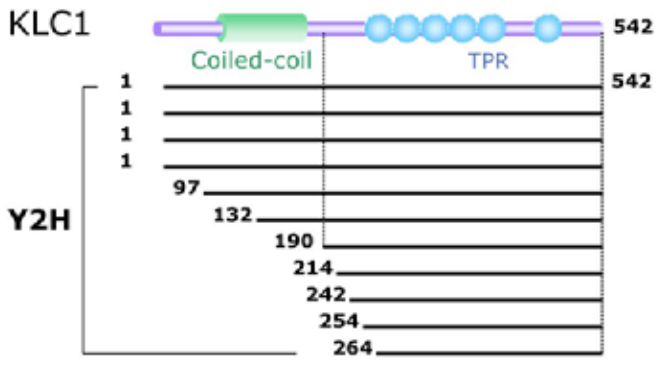
KLC1
Coiled-coil
TPR
542
1
542
1
1
1
97
132
190
214
242
254
264
Y2H

Figure S1

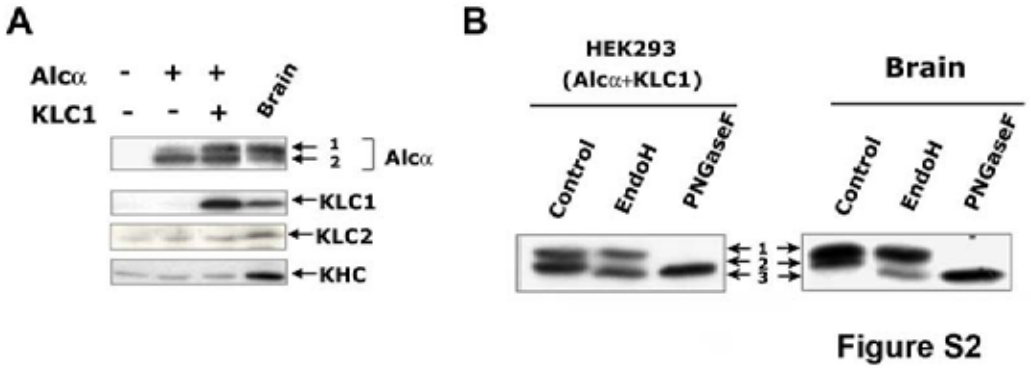
A
Alcα - + +
KLC1 - - +
Brain
1
2
Alcα
KLC1
KLC2
KHC
B
HEK293
(Alcα+KLC1)
Brain
Control
EndoH
PNGaseF
Control
EndoH
PNGaseF
1
2
3

Figure S2

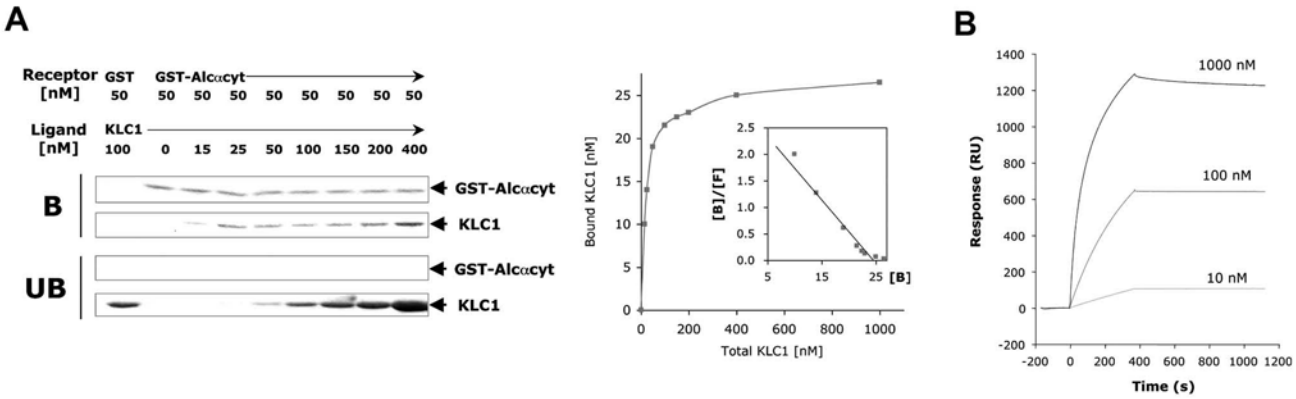
A
Receptor [nM]
GST 50
GST-Alcαcyt 50 50 50 50 50 50 50
Ligand [nM]
KLC1 100 0 15 25 50 100 150 200 400
B
GST-Alcαcyt
KLC1
UB
GST-Alcαcyt
KLC1
Bound KLC1 [nM]
Total KLC1 [nM]
[B]/[F]
[B]
B
1000 nM
100 nM
10 nM
Response (RU)
Time (s)

Figure S3

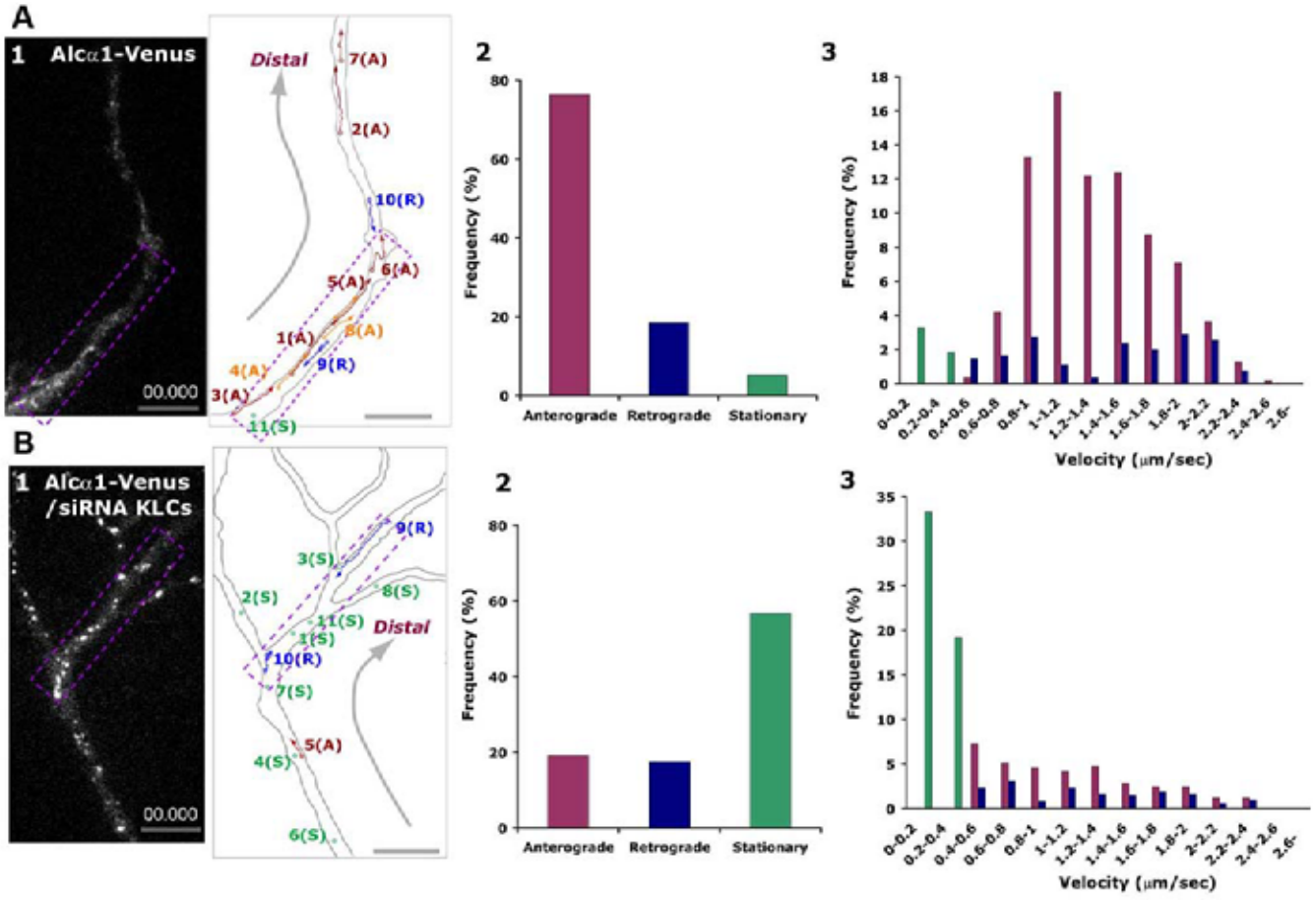
A
1 Alcα1-Venus
00.000
Distal
7(A)
2(A)
10(R)
5(A)
6(A)
1(A)
8(A)
4(A)
9(R)
3(A)
11(S)
2
Frequency (%)
Anterograde
Retrograde
Stationary
3
Frequency (%)
Velocity (μm/sec)
B
1 Alcα1-Venus /siRNA KLCs
00.000
9(R)
3(S)
2(S)
8(S)
11(S)
Distal
1(S)
10(R)
7(S)
5(A)
4(S)
6(S)
2
Frequency (%)
Anterograde
Retrograde
Stationary
3
Frequency (%)
Velocity (μm/sec)

Figure S4

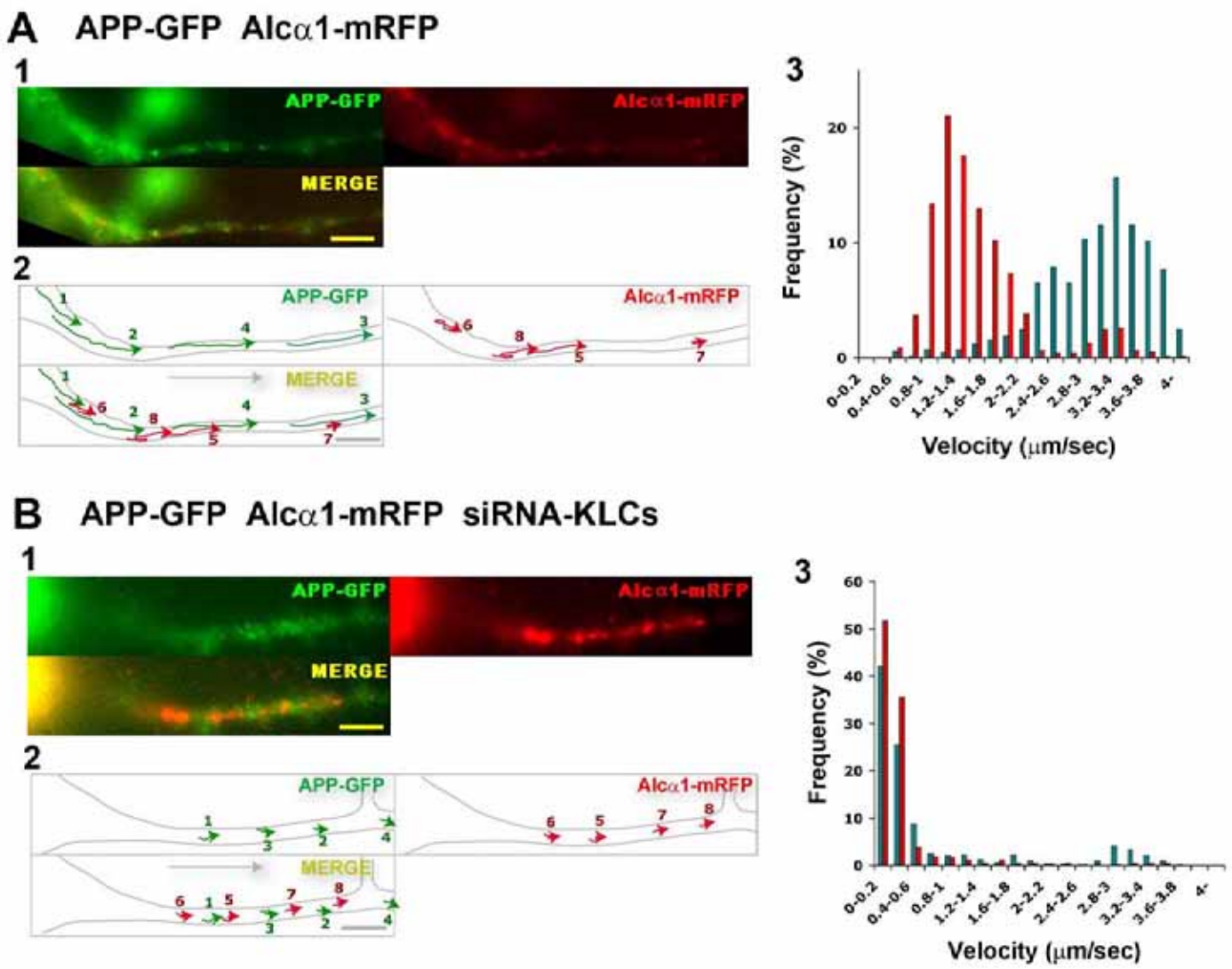
A APP-GFP Alcα1-mRFP
1
APP-GFP
Alcα1-mRFP
MERGE
2
APP-GFP
Alcα1-mRFP
MERGE
3
Frequency (%)
Velocity (μm/sec)
0-0.2
0.4-0.6
0.8-1
1.2-1.4
1.6-1.8
2-2.2
2.4-2.6
2.8-3
3.2-3.4
3.6-3.8
4-
B APP-GFP Alcα1-mRFP siRNA-KLCs
1
APP-GFP
Alcα1-mRFP
MERGE
2
APP-GFP
Alcα1-mRFP
MERGE
3
Frequency (%)
Velocity (μm/sec)

Figure S5

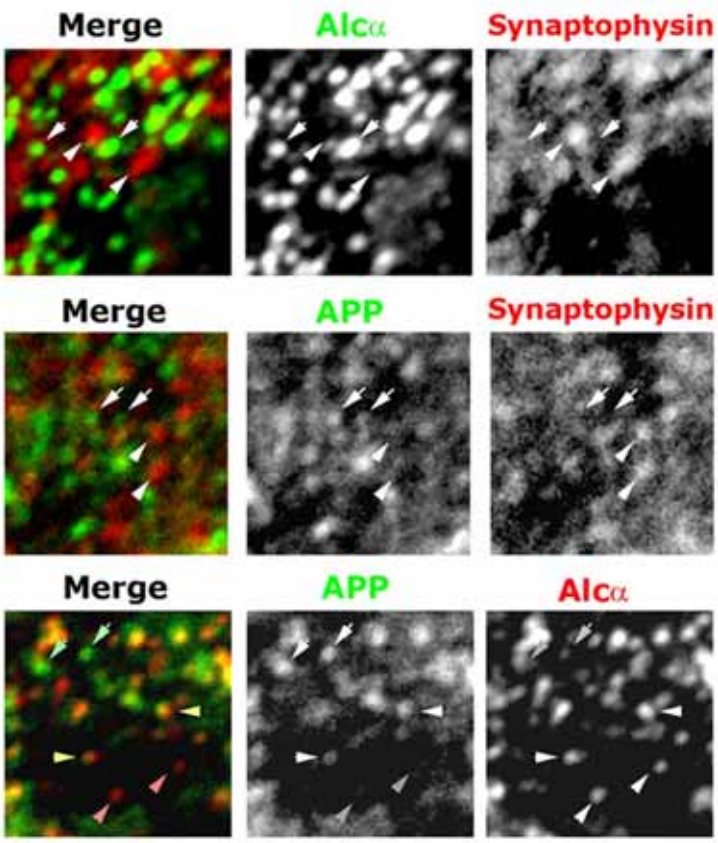
Merge
Alcα
Synaptophysin
Merge
APP
Synaptophysin
Merge
APP
Alcα

Figure S6

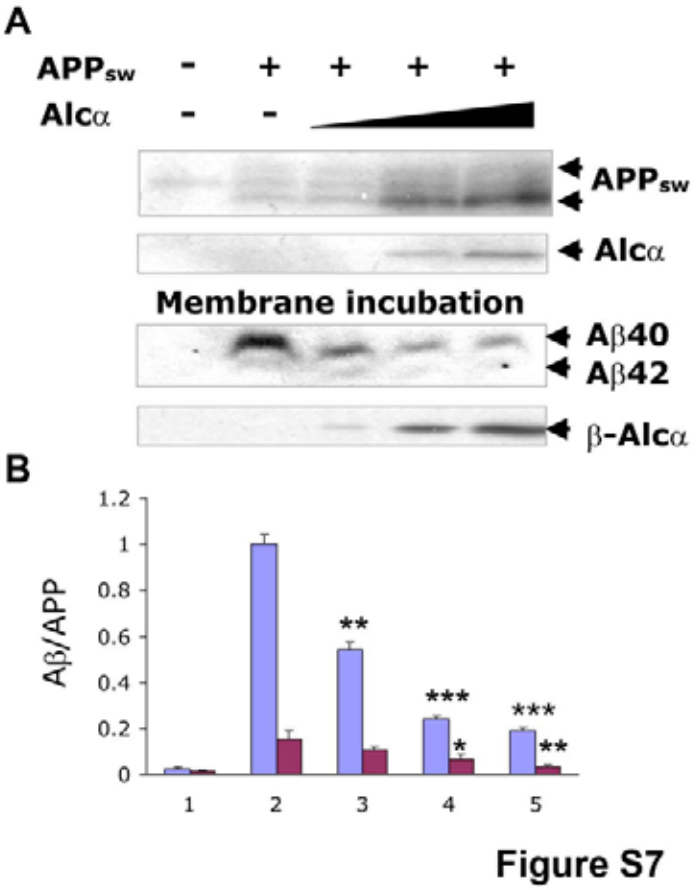
A
APPsw - + + + +
Alcα - -
APPsw
Alcα
Membrane incubation
Aβ40
Aβ42
β-Alcα
B
Aβ/APP
1.2
1
0.8
0.6
0.4
0.2
0
**
***
*
***
**
1
2
3
4
5

Figure S7

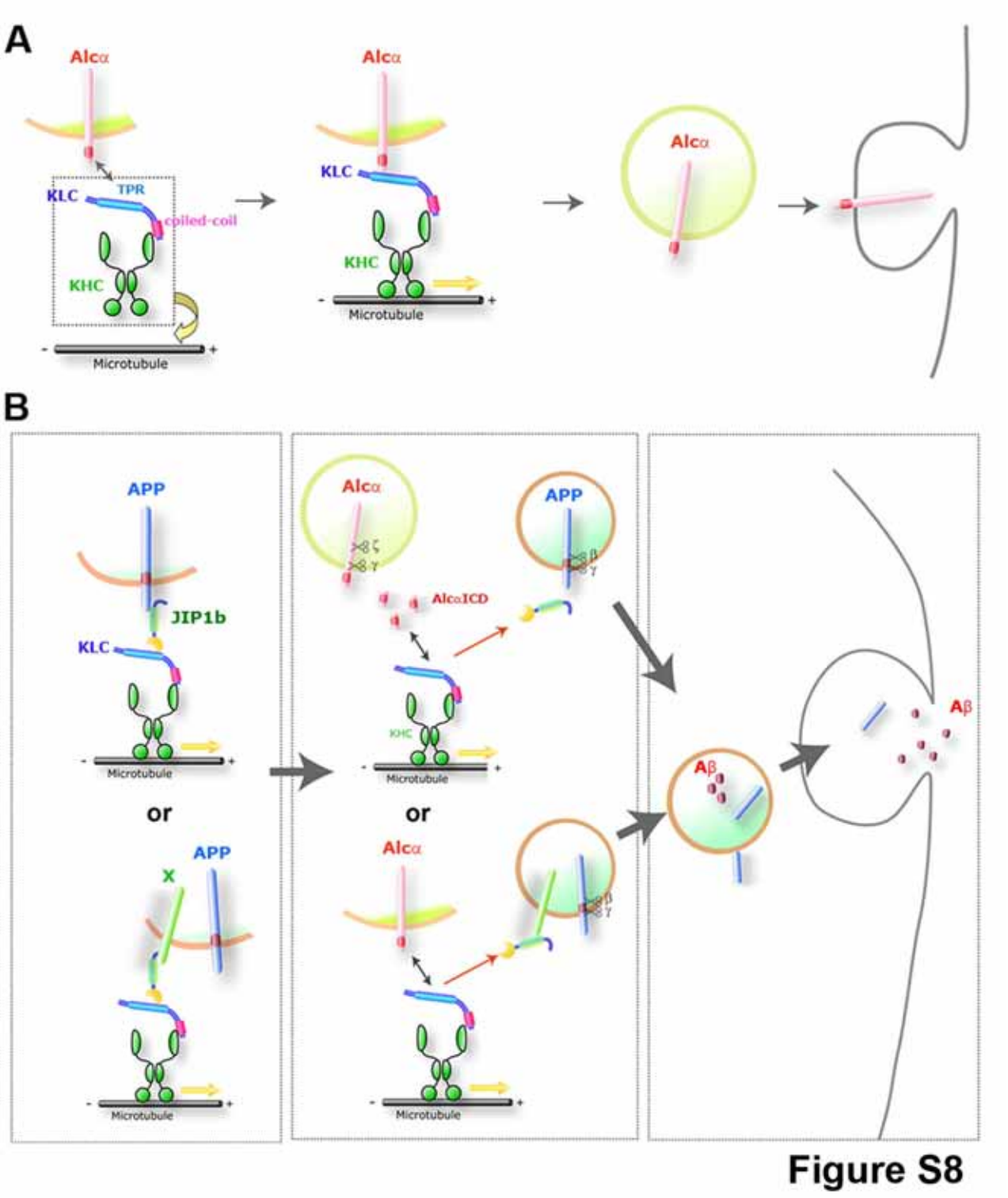
A
Alcα
TPR
KLC
coiled-coil
KHC
Microtubule
Alcα
KLC
KHC
Microtubule
Alcα
B
APP
JIP1b
KLC
Microtubule
or
APP
X
Microtubule
Alcα
APP
AlcαICD
KHC
Microtubule
or
Alcα
Microtubule
Aβ
Aβ

Figure S8

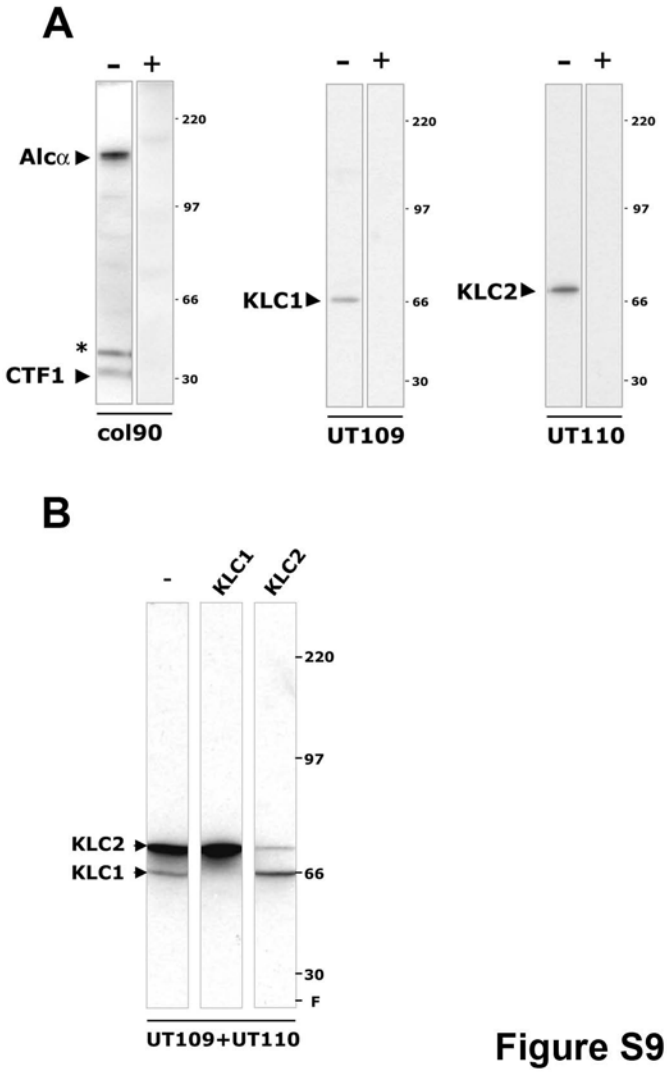
A
- +
Alcα
CTF1
*
220
97
66
30
col90
KLC1
UT109
KLC2
UT110
B
-
KLC1
KLC2
KLC2
KLC1
F
UT109+UT110

Figure S9